PFC/RR-92-15 DOE/ET-51013-298

Comparison of Alcator C Data with the Rebut-Lallia-Watkins Critical Gradient Scaling

Ian H. Hutchinson

Plasma Fusion Center
Massachusetts Institute of Technology
Cambridge, MA 02139

December 1992

This work was supported by the U. S. Department of Energy Contract No. DE-AC02-78ET51013. Reproduction, translation, publication, use and disposal, in whole or in part by or for the United States government is permitted.

Comparison of Alcator C data with the Rebut-Lallia-Watkins Critical Gradient Scaling

I.H.Hutchinson

Plasma Fusion Center
Massachusetts Institute of Technology
Cambridge, Massachusetts, USA.

Abstract

The critical temperature gradient model of Rebut, Lallia and Watkins is compared with data from Alcator C. The predicted central electron temperature is derived from the model, and a simple analytic formula is given. It is found to be in quite good agreement with the observed temperatures on Alcator C under ohmic heating conditions. However, the thermal diffusivity postulated in the model for gradients that exceed the critical is not consistent with the observed electron heating by Lower Hybrid waves.

1. Introduction

In view of the importance attached to the critical temperature gradient model [1] of tokamak transport in recent ITER design discussions, a more thorough comparison of the predictions of the model has been undertaken with the confinement observed in Alcator C.

The confinement model is summarized in section 2. Its main consequence is that the electron temperature profile is, in ohmically heated cases, close to the prescribed critical gradient. Section 3 shows how a simple but quite reliable analytic integration of this gradient can be used to derive a formula for the electron temperature, and from this the global stored energy can be obtained by simple profile assumptions. The global energy deduced is in the same form as that previously given in ref [1] but differs quantitatively.

Section 4 compares the model predictions with ohmic data from Alcator C and shows that the predictions derived from the critical gradient model are in quite good agreement with the data. Section 5 analyses the temperature rises observed in Lower Hybrid heating experiments. These are found not to be explicable by the incremental diffusivity in the model.

2. The Rebut-Lallia-Watkins Model

The critical temperature gradient model consists of two key parts, each of which is governed by an empirically chosen coefficient. The first ansatz is that there exists a critical electron temperature gradient, $|\nabla T_e|_c$, above which anomalous diffusivity of heat and particles is turned on. The second ansatz concerns the form of the anomalous electron thermal diffusivity, χ_e for gradients that exceed the critical.

The most recent published formulas [2] for these two quantities are

$$|\nabla T_e|_c = K \frac{1}{q} \sqrt{\frac{\eta j B^3}{n_e T_e^{1/2}}}, \tag{1}$$

where $K = 0.06\sqrt{e^2/\mu_0 m_e^{1/2}}$ and

$$\chi_e = 0.5c^2 \sqrt{\mu_0 m_i}(1 - \sqrt{r/R})\sqrt{1 + Z_{\text{eff}}} \left(\frac{\hat{\mathbf{r}}.\nabla T_e}{T_e} + 2\frac{\hat{\mathbf{r}}.\nabla n_e}{n_e} \right) \frac{q^2}{|\nabla q|} \frac{1}{B\sqrt{R}} \sqrt{T_e/T_i}$$
$$\times \left(1 - \frac{|\nabla T_e|_c}{|\nabla T_e|} \right) H(|\nabla T_e| - |\nabla T_e|_c) H(\hat{\mathbf{r}}.\nabla q) \tag{2}$$

Here q is the safety factor, η the resistivity, j the current density, B the toroidal magnetic field, H is the Heavyside step function, and $\hat{\mathbf{r}}.\nabla$ is the outward gradient perpendicular to the flux surface, meaning d/dr in a circular cross-section machine. (In the original publications, ∇ was used apparently to signify this signed scalar radial derivative.) All

other symbols have their conventional meanings, and are in S.I. units (temperatures in Joules).

Additional assumptions that are needed to perform complete simulations are that the anomalous ion thermal and particle diffusivities are

$$\chi_i = 2\sqrt{\frac{T_e}{T_i}}\frac{Z_i}{\sqrt{1+Z_{\rm eff}}}\chi_e \tag{3}$$

and

$$D_i = 0.7\chi_i. \tag{4}$$

Also the neoclassical coefficients should be added to the anomalous transport coefficients, although the extra contributions are generally small and will be ignored here.

The earlier publication [1] gave identical critical gradient but the expression for the electron thermal diffusivity was different, being equal to that in Eq. (2) times the factor

$$0.3\frac{R}{r}\frac{1}{(1-\sqrt{r/R})\sqrt{1+Z_{\rm eff}}}, \tag{5}$$

which is not much different from unity in typical cases. In addition, reference [1] gave a global scaling law for the electron energy that was said to be "consistent with" these expressions and can be written as

$$W_{cg} = 0.15 n_{20}^{3/4} Z_{\rm eff}^{1/4} B^{1/2} I_M^{1/2} (Rab)^{11/12} + 1.2\times 10^{-2} I_M (Rab)^{1/2} P_M / Z_{\rm eff}^{1/2} \qquad \text{MJ}, \tag{6}$$

where n_{20} is the electron density in units of 10^{20} m^{-3}, I_M is the plasma current in MA, a is the minor radius, b is the plasma half-height, and P_M is the total heating power in MW. Rebut *et al* recommend that this global law should be used only as a general guide.

3. Integration of the Gradient

Since there is no detailed profile information in the Alcator C database, the most reasonable comparison that can be made is with the electron temperature measurements and the global confinement information. A comparison of experimental profiles with those simulated using the above coefficients is not feasible. Comparisons with the global expression Eq. (6) will be given. However, a more faithful representation of the critical gradient model in global terms is derived first, and proves to be a better fit to the experiment.

When the total heating power is small, the expectation is that the electron temperature profile will adjust so as to be exactly at the critical threshold. In such a case the electron temperature can be obtained by integrating Eq. (1) inward from the edge (where we shall take T_e to be negligible). In a circular cross-section plasma the gradient is just d/dr and its strongest radial variation arises from the variation of $1/q$. In a steady-state situation,

where bootstrap current or non-inductive current drive can be ignored, ηj is independent of r. The weaker variation with n_e and T_e can be taken into account in the integration by approximating the density profile shape to be proportional to the temperature profile shape to a power γ, i.e. $n_e/n_{e0} = (T_e/T_{e0})^\gamma$, where subscript zero refers to the central value (also equal to the value at the $q = 1$ radius in a model where sawteeth flatten the profile). Then the equation governing T_e is

$$T_e^{(1/4+\gamma/2)} \frac{dT_e}{dr} = -A T_{e0}^{(1/4+\gamma/2)} \frac{1}{q}, \tag{7}$$

where $A = K\sqrt{\eta j B^3/(n_{e0} T_{e0}^{1/2})}$ is independent of r. This equation can be integrated to obtain

$$T_e(r)^{(5/4+\gamma)} = (5/4 + \gamma/2) A T_{e0}^{(1/4+\gamma/2)} \int_r^a \frac{1}{q} dr. \tag{8}$$

In a full numerical solution, the q-profile is determined self-consistently from the temperature profile. However, various *ad hoc* effects such as sawteeth must also be included. Therefore it is reasonable to adopt a model q-profile which is easy to deal with analytically. The form we adopt here is $1/q = 1 - (1 - 1/q_a)(r - r_0)/(a - r_0)$, i.e. linear variation of $1/q$ from the $q = 1$ radius r_0 to its edge value $1/q_a$. This gives a curvature to the q-profile similar to what is observed experimentally. Then the integral is straightforward and applying Eq.(8) at radius r_0 we get

$$T_{e0} = T_{ec} = (5/4 + \gamma/2) A (a - r_0)(1 + 1/q_a)/2 \tag{9}$$

We shall take T_e to be flat within the radius r_0. Figure 1 illustrates the profile shapes of q, which is assumed, and T_e which is derived, in the case $q_a = 4$.

Now the coefficient A contains variation with T_{ec} which must be included to obtain the final solution. For simplicity, and since the published model does not specify it, we shall take the resistivity to be Spitzer: $\eta = \eta_1 Z_\sigma T_e^{-3/2}$, where η_1 is a constant (ignoring coulomb logarithm variations) and Z_σ represents the resistivity variation due to impurities (which, contrary to frequent assumption, is not simply $Z_{\rm eff}$). Also the current density at the $q = 1$ surface is $j = 2B/\mu_0 R$. Making these substitutions we obtain

$$T_{ec} = K^{1/2} (2\eta_1/\mu_0)^{1/4} [(5/4 + \gamma/2)(1 - r_0/a)(1 + 1/q_a)/2]^{1/2} Z_\sigma^{1/4} n_{e0}^{3/4} R^{-1/4} a^{1/2} B. \tag{10}$$

It is found empirically in a wide range of tokamak experiments that the radius of the $q = 1$ surface is given quite well by $r_0 = a/q_a$. In that case the dependence of Eq. (10) on the edge q is weak, proportional to $(1 - 1/q_a^2)^{1/2}$. Also, generally, the density profile is rather flatter than the temperature, $\gamma \lesssim 0.5$. Therefore the entire square bracket expression

is nearly a constant, which, when the square root is taken, becomes approximately 0.9. Substituting also for the other constants, and converting to convenient units, we obtain

$$T_{ck} = 0.5 Z_o^{1/4} n_{20}^{-1/4} R^{-1/4} a^{1/2} B, \tag{11}$$

where T_{ck} is the central temperature in keV and n_{20} refers to the central density. (For elongated plasmas one should replace a in this expression with $(ab)^{1/2}$.)

In order to conduct out the heat, the temperature gradient must be somewhat above the critical value, thus the temperature is somewhat higher than Eq. (11). In order to derive this temperature increment we equate the conduction heat flux derived from Eq (2) to the heating power. Because of the form of χ_e in Eq. (2), the heat flux equation can be written

$$|\nabla T_e| = |\nabla T_e|_c + Q/\kappa_t, \tag{12}$$

where Q is the heat flux density, equal to the total heating power divided by surface area (in steady state), and

$$\kappa_t = 0.5 c^2 \sqrt{\mu_0 m_i} \left(1 - \sqrt{\frac{r}{R}}\right) \left(\frac{\hat{\mathbf{r}}.\nabla T_e}{T_e} + 2\frac{\hat{\mathbf{r}}.\nabla n_e}{n_e}\right) \frac{q^2}{|\nabla q|} \frac{1}{B\sqrt{R}} n_e$$
$$\times \left(\sqrt{1+Z_{\rm eff}} \sqrt{\frac{T_e}{T_i}} + \sum_i 2\frac{n_i Z_i}{n_e} \frac{T_e \hat{\mathbf{r}}.\nabla T_i}{\hat{\mathbf{r}}.\nabla T_e T_i}\right). \tag{13}$$

In this expression the electron and ion contributions to the heat conductivity correspond to the first and second terms in the final parentheses.

Clearly, rather sweeping simplifications are necessary to obtain analytic solutions to Eq (12). However, since the central electron temperature is given by the radial integral of this equation, a substitution of average values in the expressions for Q and κ_t will give quite a good approximation. We adopt the following approach. First the ion and electron temperature profile shapes are taken the same. This reduces the final term to $(\sqrt{(1+Z_{\rm eff})T_e/T_i} + 2)$. Second the gradient scale lengths are replaced with constants as follows: $\hat{\mathbf{r}}.\nabla T_e/T_e \equiv 1/L_T$, $\hat{\mathbf{r}}.\nabla n_e/n_e \equiv 1/L_n$, $|\nabla q|/q^2 \equiv 1/(q_a L_q)$. Finally everything else is taken to have an appropriate average value.

When the equation is then integrated, the first term corresponds to Eq (9), which may be written $C(a-r_0)/T_{e0}$, bringing out the temperature dependence explicitly. Then we get:

$$T_{e0} = \frac{C(a-r_0)}{T_{e0}} + \frac{Q(a-r_0)}{\kappa_t}, \tag{14}$$

a quadratic equation for T_{e0}. Provided the second term is small the solution may be written $T_{e0} \approx T_{ec} + Q(a-r_0)/2\kappa_t$, where T_{ec} is the critical-gradient central temperature of Eq. (10).

The heat flux may be approximated by dividing the heating power, P_t, by the surface area, and then the increment to the central temperature, may be written

$$\frac{Q(a-r_0)}{2\kappa_t} = \frac{6.1\times10^{-3} \quad BP_t(1-r_0/a)}{\sqrt{A_i}(1-\sqrt{r/R})(1/L_t+2/L_n)L_q q_a(\sqrt{(1+Z_{\rm eff})T_e/T_i}+2)n_e}, \tag{15}$$

where A_i is the ion mass number.

For the purposes of obtaining general results, we shall take typical profile quantities as follows $L_q q_a = a$, $L_t = a$, $L_n = 2a$, $1-\sqrt{r/R} = 0.6$, and $1-r_0/a = 1-1/q_a$. Then converting to practical units and adding to the critical gradient term gives the electron temperature in keV as

$$T_{e0} = 0.5\frac{Z_\sigma^{1/4}a^{1/2}B}{R^{1/4}n_{20}^{1/4}} + \frac{0.32 \quad (1-1/q_a)}{\sqrt{A_i}(\sqrt{(1+Z_{\rm eff})T_e/T_i}+2)}\frac{BP_M}{R^{1/2}n_{20}}. \tag{16}$$

The electron energy content of the plasma is then 3/2 times the volume times the average electron pressure. The temperature profile is, in principle, available from the previous equations. However, it is more convenient, and gives negligible error compared to other uncertainties, to use a simple temperature profile shape, consistent with experiment and with Spitzer resistivity, namely $T_{e0}(1+r^2/a^2)^\alpha$, with $\alpha = 2(q_a-1)/3$. This then gives rise to a mean electron pressure equal to $n_{e0}T_{e0}/(1+\alpha(1+\gamma))$. Fixing the density profile index as $\alpha\gamma = 0.5$, since its effect is not very strong, we get the electron kinetic energy in MJ:

$$\begin{aligned} W'_{cg} &= 1.6\times10^{-2}[9/(7+4q_a)]2\pi R\pi a^2 n_{20}T_{e0} \\ &= \frac{0.20}{(1+0.57q_a)}Z_\sigma^{1/4}n_{20}^{3/4}R^{3/4}a^{5/2}B + \frac{0.13}{(1+0.57q_a)}\frac{(1-1/q_a)BP_MR^{1/2}a^2}{\sqrt{A_i}(\sqrt{(1+Z_{\rm eff})T_e/T_i}+2)}. \end{aligned} \tag{17}$$

In this equation, and equation (16) for the central temperature, the second term is a less reliable representation of the critical gradient model than the first. However, this second term is relatively small for the entire Alcator C ohmic database. So any uncertainties arising from the approximations we have introduced should not give large errors in the predictions.

Our expression, Eq. (17), can be compared with the global expression given by Rebut *et al*, Eq. (6). The ratio of the 'offset' (i.e. first) terms of Eq. (17) and Eq. (6) is $0.6(R/a)^{1/3}(Z_\sigma/Z_{\rm eff})^{1/4}\sqrt{q_a}/(1+0.57q_a)$ which is somewhat smaller than one, for example about 0.6 when $q_a = 4$ and $R/a = 4$ and $Z_{\rm eff} = 1$. The ratio of the 'linear' (i.e. second) terms is

$$2.2\frac{q_a-1}{1+0.57q_a}\frac{R}{a}\frac{Z_{\rm eff}^{1/2}}{\sqrt{A_i}(\sqrt{(1+Z_{\rm eff})T_e/T_i}+2)}$$

which is rather larger than one, about 1.4 for the above example parameters and $T_e/T_i = 1.4$ and $A_i = 2$. Thus the global expression is approximately confirmed, but there are significant differences in the offset term and the relative importance of the linear term is greater in the present expression, Eq. (17).

4. Comparison with Alcator C ohmic heating results

An extensive database exists of over 1000 ohmic shots on Alcator C [3]. The majority of these are for the standard size (R = 0.64 m, a = 0.165 m) limited plasmas. Some are of the alternate major radius plasmas (0.58 and 0.7 m) that helped to establish NeoAlcator scaling [4]. Fields range from about 6 to 12 tesla, currents from about 0.1 to 0.8 MA, densities from about 0.5 to 8 $\times 10^{20}$, and energy confinement times from 0.0025 to 0.05 s. Approximately 60 shots had pellet fuelling.

The formulas of the previous section can be applied directly to the data in this database. The resistivity factor Z_σ is deduced from the loop voltage (and used in place of $Z_{\rm eff}$).

For the entire database, the ratio of the linear (second) term to the total expression of Rebut *et al*'s global electron energy, Eq. (6), has an average value of 2.3%, and never exceeds 7%. In the present representation of the critical gradient model, Eq. (17), the ratio has an average value of 9% and a maximum of 28%. Thus the ohmic confinement is mostly dominated by the offset term. In the physical context of the model, this means that the electron temperature should always be close to the critical gradient.

The central electron temperature is predicted quite well by Eq. (16) as is illustrated in Fig 2. This is the most direct test of the critical temperature gradient expression, and in essence any other comparisons are an elaboration, since deriving the stored energy from the central temperature is mostly a matter of profiles. Many of the outliers are hydrogen points, that generally give slightly worse performance in practice but whose model prediction is increased by the $1/\sqrt{A_i}$ factor in the linear term.

The agreement is confirmed by Fig. 3, which compares the measured stored energy with Eq. (17). The revised critical gradient scaling slightly overpredicts the actual results. However, the agreement is really quite good, especially since these plots are on a *linear* scale, not logarithmic.

The agreement with the original global energy scaling of Rebut, Lallia and Watkins (Eq. (6)) is not as good, as illustrated by Fig. 4, because their global expression does not represent the critical gradient model for the electron temperature so well. This scaling predicts energy higher than that observed, by a factor of approximately two. More significantly, perhaps, it is found that the current variation of this scaling is systematically different from the experimental data. Fig. 5 illustrates this by plotting the ratio of observed energy to Eq. (6) versus plasma current. The observed energy increase with current

is substantially less than that of the scaling. This is the main systematic discrepancy that can be discovered in the data. The revised critical gradient scaling removes most of that discrepancy, as illustrated by Fig. 6.

5. Comparison with Alcator C Lower Hybrid heating results

The Alcator C program included substantial auxiliary heating experiments with over 1 MW of Lower Hybrid power at 4.6 GHz. These were in addition to the extensive current drive campaigns [5,6]. Two main series of heating experiments were conducted. The first [7], with SiC coated graphite limiters observed large electron temperature increases, but was complicated by serious carbon influxes that greatly increased the $Z_{\rm eff}$. The second [8], with Molybdenum limiters again saw substantial temperature rises, but were able to minimize the impurity impact. Only modest $Z_{\rm eff}$ increases were observed, and the heating could unambiguously be attributed to the electron Landau damping expected. These are, of course, *electron* heating experiments.

Since a systematic database of data from these experiments is not available, comparisons have been made of two typical shots, with and without the heating, from these two campaigns. There were numerous similar shots, and the data has been drawn from published material [7,8].

The great advantage of these experiments is that good control of the electron density was maintained, unlike many of today's more ambitious experiments. Therefore we can be confident that the only bulk parameter that changes in these shots, in addition to the heating power and temperature, is the $Z_{\rm eff}$. All the parameters needed for evaluation of the critical gradient prediction of the electron temperature were measured. Therefore a direct comparison is possible.

The data are shown in Table 1. The additional parameters are $B = 5.5$ T, $I_p = 0.26$ MA, $n_e = 1.4 \times 10^{20}$ m^{-3} for the molybdenum limiter cases and $B = 9$ T, $I_p = 0.4$ MA, $n_e = 1.3 \times 10^{20}$ m^{-3} for the SiC limiter cases. Fractional increases in the electron temperature of 0.5 and 0.65 respectively were observed. However, the fractional increases predicted by Eq. (16), the critical gradient model, are only 0.21 and 0.35 respectively. The comparison is even less favorable for the global energy (W_{cg}) expression of Rebut *et al*, Eq. (6). Fractional electron energy increases of 0.13 and 0.31 are predicted.

In Table 1 the contributions from the offset and the linear terms are given separately. These show that in W_{cg} the linear term is still negligible, and the predicted increase, due to $Z_{\rm eff}$ influence in the offset term, is inadequate by at least a factor of two to explain the observed heating. The critical temperature gradient T_e prediction shows non-negligible contribution to the temperature increase (0.1 to 0.15 of T_e) from the linear term. But this is still unable to explain what is observed, even with the additional $Z_{\rm eff}$ effects.

If one were arbitrarily to increase the coefficient of the linear term, via a decrease of the anomalous χ by some factor, it would be necessary for this increase factor to be 4.0 and 6.6 , for Mo and SiC limiters respectively, to give the correct T_e ratio with and without LH heating. This would exacerbate the overprediction of the absolute temperature, so one would be forced to decrease the offset coefficient simultaneously. In any case, the required change in the ratio of the linear to the offset terms would remain the same (4.0 or 6.6). This factor is certainly outside the uncertainty in the coefficients arising from the profile approximations that have been made. We can therefore conclude that the published critical gradient model is not consistent with the Alcator C Lower Hybrid heating results.

Acknowledgement

Work supported by U.S.DOE Contract No. DE-AC02-78ET51013.

References

[1] P-H.Rebut, P.P.Lallia, and M.L.Watkins, in *Plasma Physics and Controlled Nuclear Fusion Research*, Nice, 1988 (IAEA, Vienna 1989) Vol 2, p191.

[2] P-H.Rebut, M.L.Watkins, D.L.Gambier, and D. Boucher, Phys. Fluids B **3**, 2209 (1991).

[3] S.M.Wolfe, private communication.

[4] B.Blackwell *et al.* in *Plasma Physics and Controlled Nuclear Fusion Research*, Baltimore, 1982, (IAEA, Vienna, 1982) Vol 2, p27.

[5] S.Knowlton, *et al.*, Phys. Rev. Lett. **57**, 587 (1986).

[6] Y.Takase, *et al.*, Nucl. Fusion, **25**, 53 (1987).

[7] M.Porkolab, *et al.*, Phys. Rev. Lett. **53**, 1229 (1984).

[8] M.Porkolab, *et al.*, in *Plasma Physics and Controlled Nuclear Fusion Research*, Kyoto, 1986, (IAEA, Vienna, 1987) Vol 1, p509.

Experiment	Mo-Limiter		Ratio	SiC-Limiter		Ratio
P_{rf}, MW	0	1.0		0	1.0	
V_l, volts	1.8	1.3		1.7	2.0	
Z_{eff}	1.5	2.1		1.6	4.5	
T_i, keV	0.85	1.1		1.0	1.85	
T_{eo}, keV	1.2	1.8	1.5	2.0	3.3	1.65
Model Prediction			Ratio			Ratio
T_e, keV	1.27+0.10	1.38+0.28	1.21	2.15+0.25	2.71+0.54	1.35
W_{cg}, kJ	6.20+0.16	6.80+0.38	1.13	9.50+0.34	12.3+0.53	1.31

Table 1. Comparison of observed Lower Hybrid heating with the Critical Temperature Gradient model. T_e from Eq. (16), W_{cg} from Eq. (6).

Figure Captions

1. Profile of the safety factor assumed, and of the resultant temperature profile from integration of the critical gradient, Eq. (8), (solid line) and (schematically) the increment arising from the anomalous χ_e (dashed line).
2. Comparison of the central electron temperature predicted by Eq. (16) with the Alcator C ohmic database.
3. Comparison of the total stored electron energy predicted by Eq. (17) with the experimentally observed values in Alcator C.
4. Comparison of the global stored electron energy scaling given in reference [1], (Eq. (6)) with the Alcator C data.
5. Ratio of the observed stored energy to the RLW global scaling (Eq. (6)) versus plasma current. A systematic trend is visible.
6. Ratio of the observed central temperature to that predicted from the critical gradient model (Eq.(16)). Most of the systematic trend with plasma current is removed.

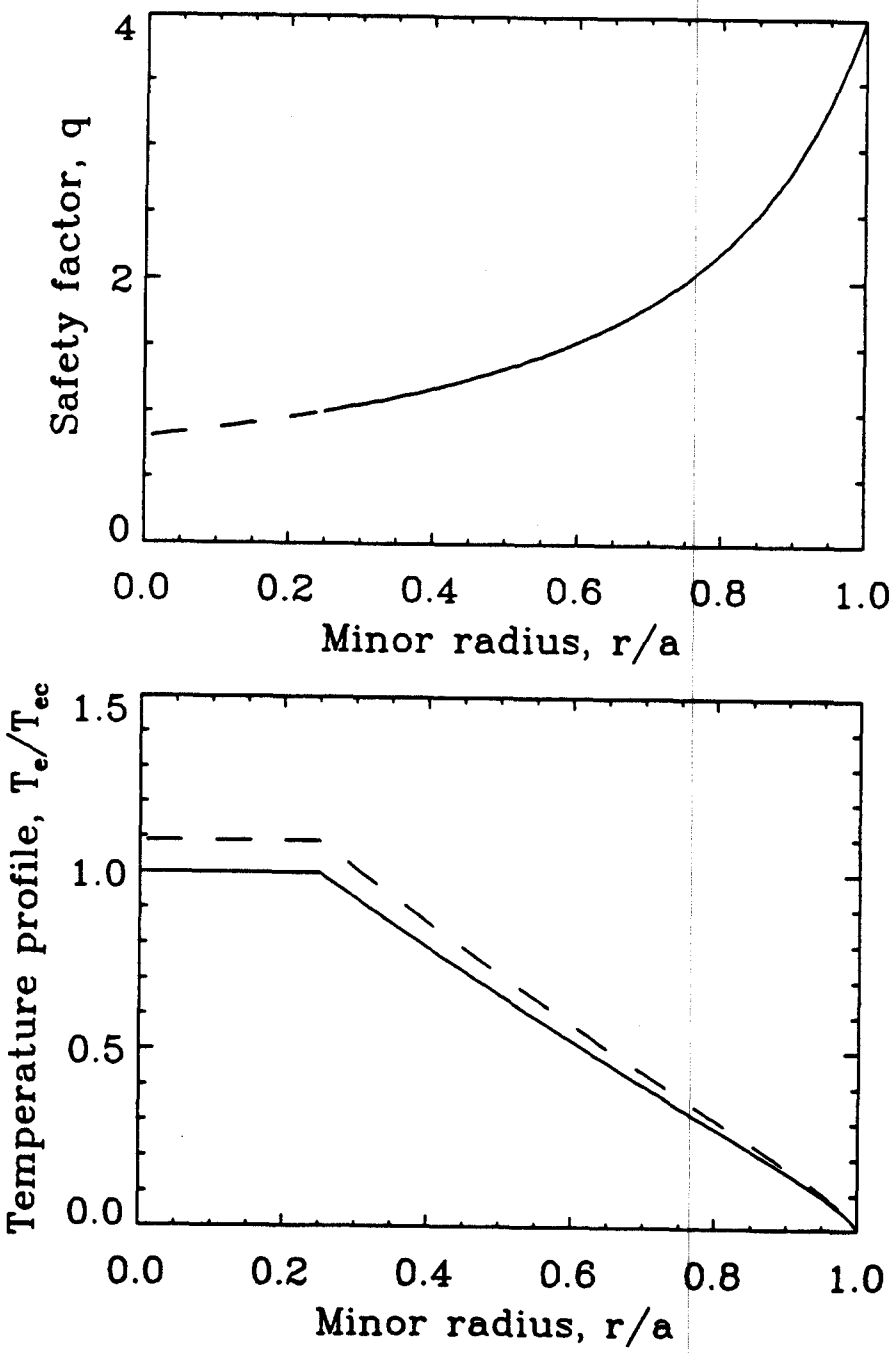

1. Profile of the safety factor assumed, and of the resultant temperature profile from integration of the critical gradient, Eq. (8), (solid line) and (schematically) the increment arising from the anomalous χ_e (dashed line).

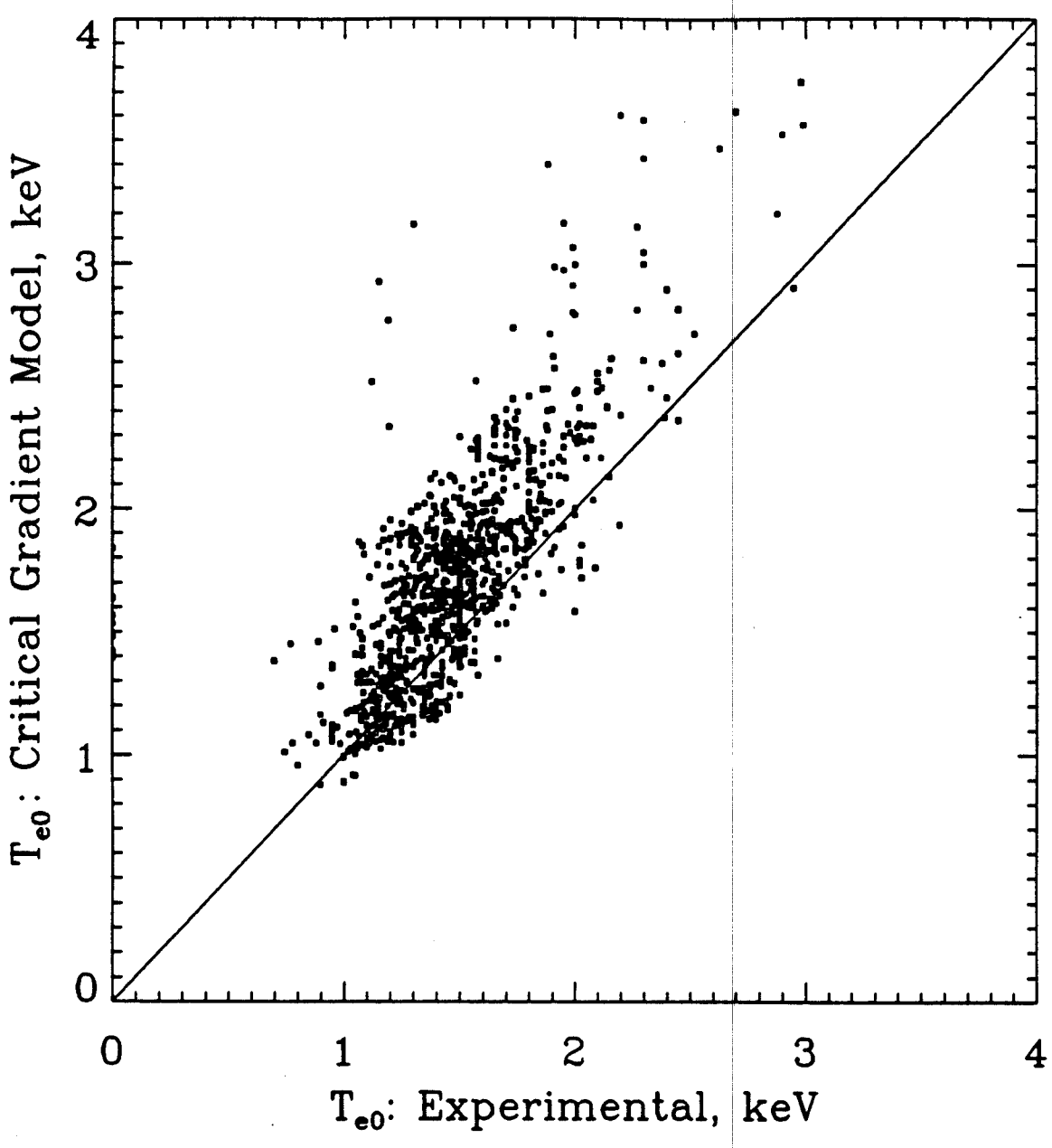

2. Comparison of the central electron temperature predicted by Eq. (16) with the Alca C ohmic database.

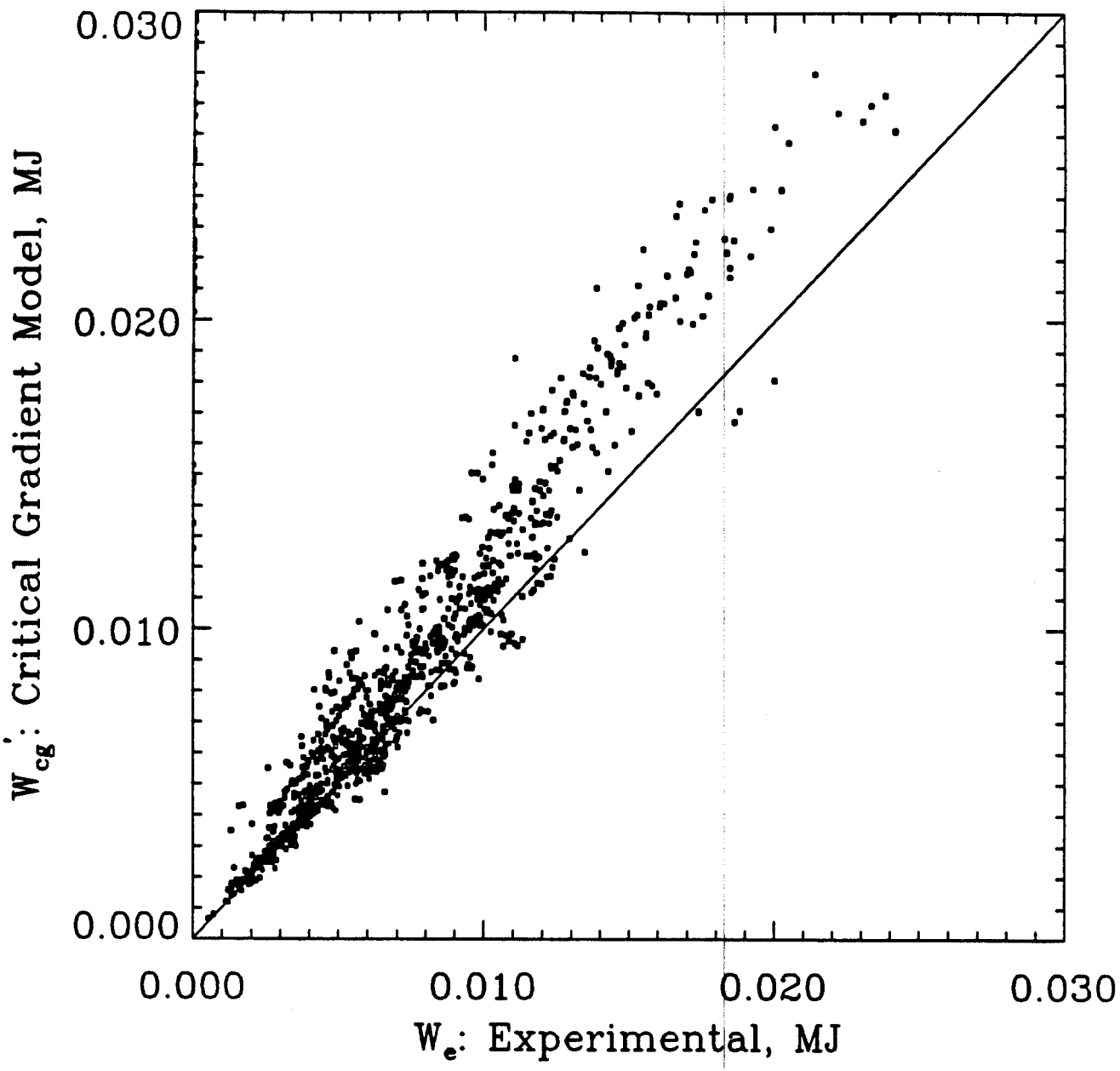

3. Comparison of the total stored electron energy predicted by Eq. (17) with the experimentally observed values in Alcator C.

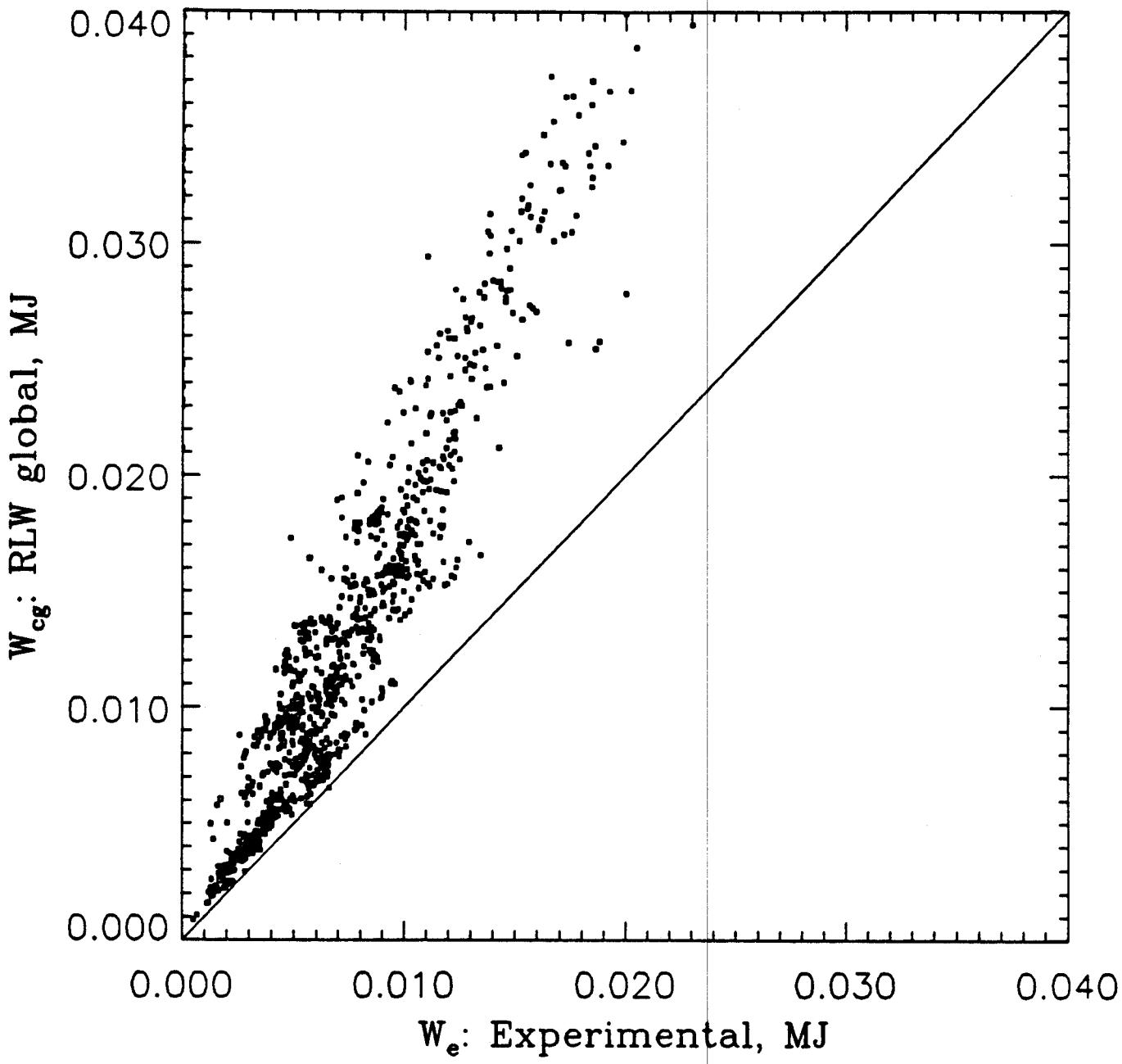

4. Comparison of the global stored electron energy scaling given in reference [1], (Eq. (6)) with the Alcator C data.

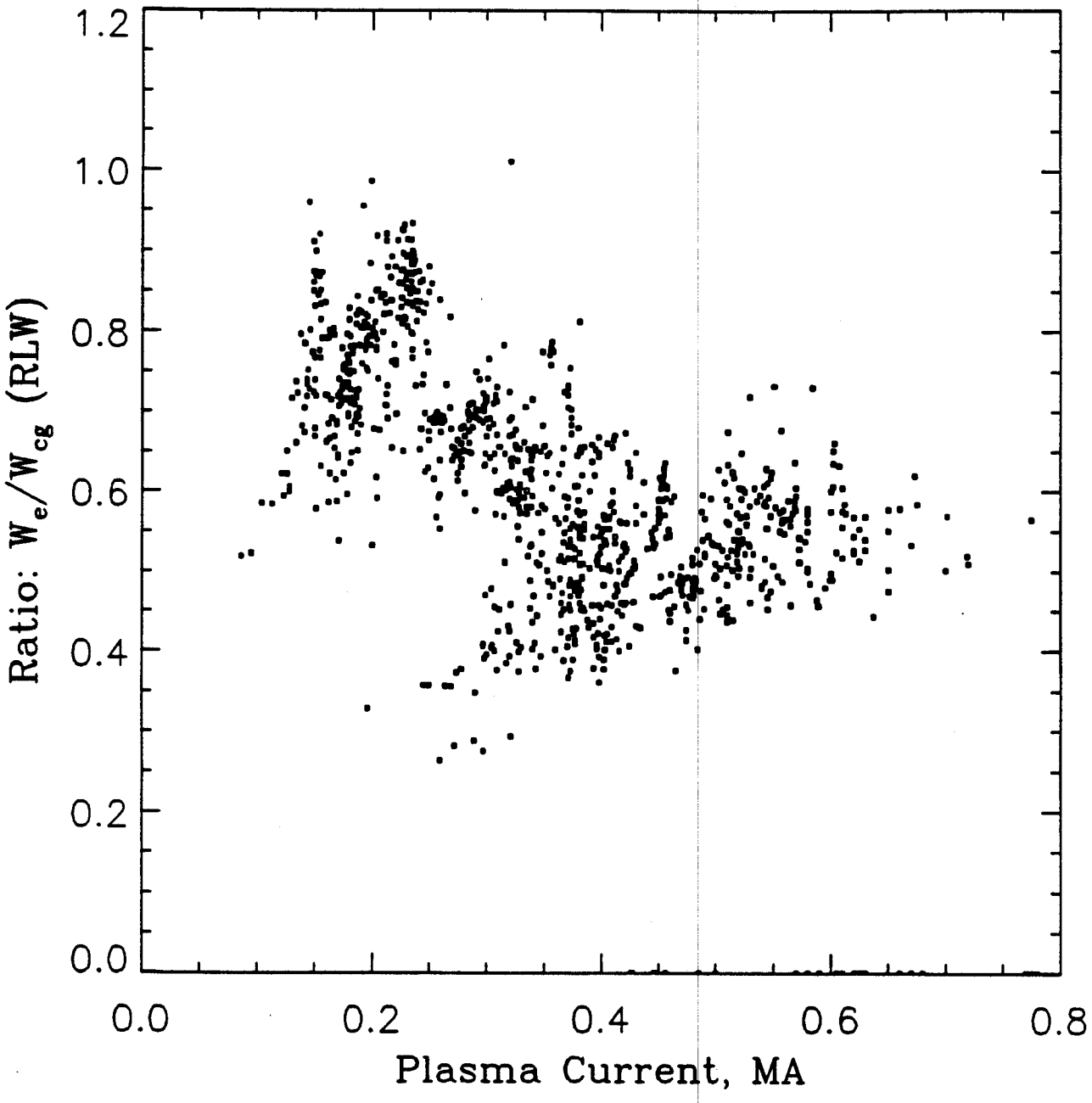

5. Ratio of the observed stored energy to the RLW global scaling (Eq. (6)) versus plasma current. A systematic trend is visible.

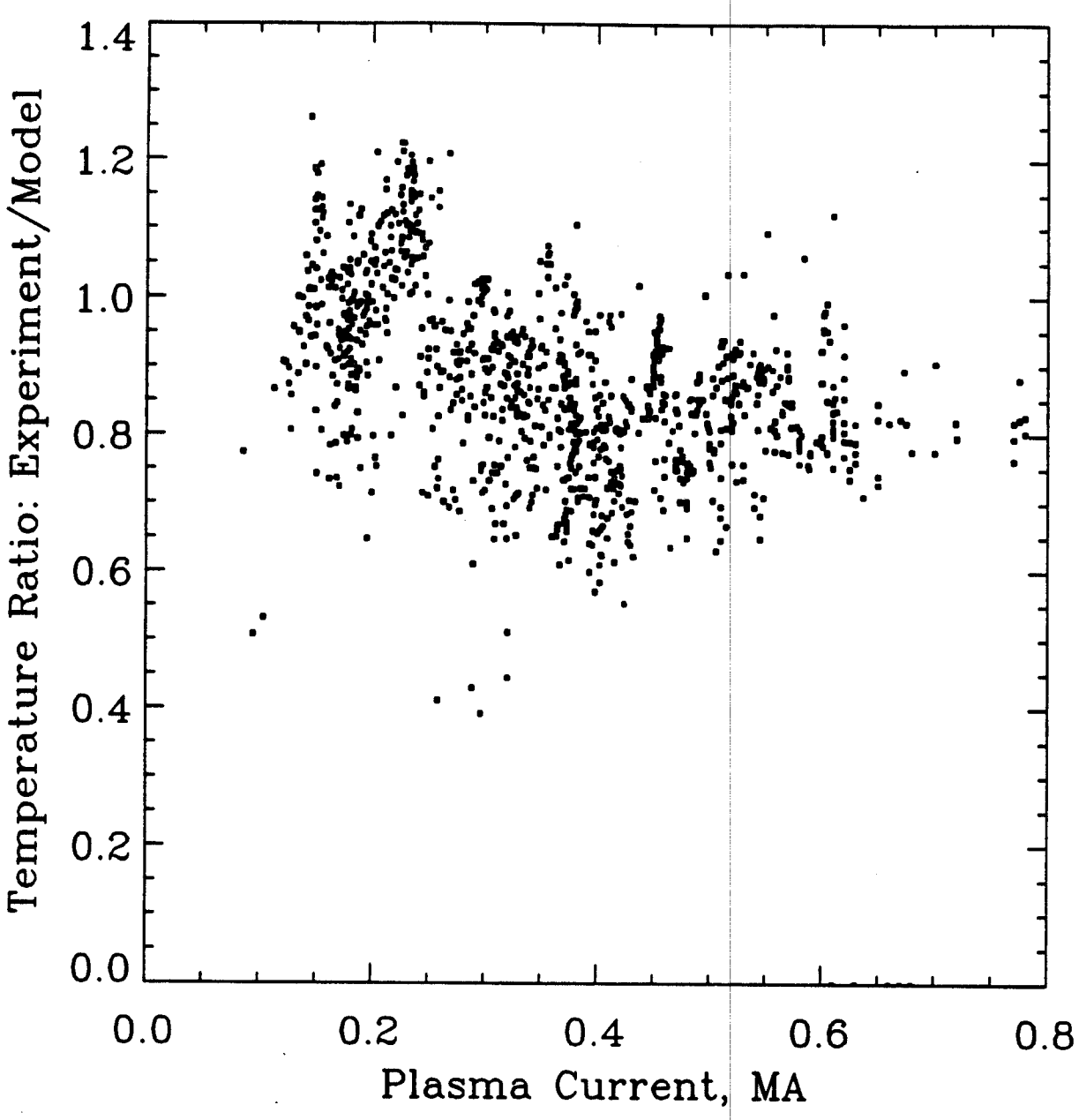

6. Ratio of the observed central temperature to that predicted from the critical gradient model (Eq.(16)). Most of the systematic trend with plasma current is removed.